



Published in final edited form as:

Sci Transl Med. 2015 May 20; 7(288): 288ra77. doi:10.1126/scitranslmed.aaa3575.

The Cytoplasmic Prolyl-tRNA Synthetase of the Malaria Parasite is a Dual-Stage Target for Drug Development

Jonathan D. Herman^{†,1,2,3,4,5}, Lauren R. Pepper^{†,6}, Joseph F. Cortese¹, Guillermina Estiu^{7,8,#}, Kevin Galinsky¹, Vanessa Zuzarte-Luis⁹, Emily R. Derbyshire¹², Ulf Ribacke², Amanda K. Lukens^{1,2}, Sofia A. Santos^{10,11}, Vishal Patel¹², Clary B. Clish¹, William J. Sullivan Jr.¹³, Huihao Zhou¹⁴, Selina E. Bopp², Paul Schimmel^{14,15}, Susan Lindquist^{6,16}, Jon Clardy^{1,12}, Maria M. Mota⁹, Tracy L. Keller¹⁷, Malcolm Whitman¹⁷, Olaf Wiest^{7,8,18}, Dyann F. Wirth^{*,1,2}, and Ralph Mazitschek^{*,1,2,10}

*To whom correspondence should be addressed: Ralph Mazitschek, Center for Systems Biology, Massachusetts General Hospital, 185 Cambridge Street, Boston, MA 02114, rmazitschek@mgh.harvard.edu, Dyann F. Wirth, Department of Immunology and Infectious Disease, Harvard School of Public Health, 665 Huntington Ave, Boston, MA 02113, dfwirth@hsph.harvard.edu.

#Deceased May 9, 2014

†Contributed equally

Supplementary Materials.

Materials and Methods

Fig. S1. High resolution melt assay of *PfcPRS* identifies mutant loci.

Fig. S2. Halofuginone is not cross-resistant with common anti-antimalarials.

Fig. S3. Proline-dependent sensitivity of *P. falciparum* to halofuginone

Fig. S4. Transgenic *S. cerevisiae* expressing wild type *PfcPRS* is sensitive to halofuginone.

Fig. S5. Proline-dependent sensitivity of transgenic *S. cerevisiae* to halofuginone

Fig. S6. Amino Acid Response Pathway

Fig. S7. Quantification of p-eIF2 α protein levels in fig. 2C

Fig. S8. Multiple protein sequence alignment of the Class II Core Domains of Proline tRNA Synthetases from diverse species.

Fig. S9. Comparison of MD studies models comparing the impact of the L482F and L482H mutations in *PfcPRS*.

Fig. S10. Proposed mechanism for halofuginone epimerization.

Fig. S11. Sensitivity of *S. cerevisiae* model strains to halofuginone.

Fig. S12. Induction of eIF2 α phosphorylation by halofuginol.

Fig. S13. Necropsy of halofuginol and vehicle treated mice.

Fig. S14. *In vivo* potency of halofuginone in liver stage *P. berghei* infection model.

Table S1. EC₅₀ values of febrifugine and analogs for erythrocytic stage 3D7, Dd2 wild-type and Dd2 halofuginone-resistant strains.

Table S2. Source data for fig. 5A

Table S3. Source data for fig. 5B

Table S4. Source data for fig. 5C

Table S5. Source data for fig. S14

Author contributions:

J.D.H., L.R.P., A.K.L., S.E.B., D.F.W. and R.M. wrote the manuscript, D.F.W. and R.M. designed the study with input from J.D.H. and L.R.P.; J.D.H. performed in vitro blood stage Plasmodium culture experiments (resistance selection, drug-profiling, mechanistic studies, PCR, Western-blot analysis), L.R.P. performed all yeast related experiments, J.F.C. performed selection experiments, G.E. performed modeling studies, K.G. performed sequencing analysis, V.Z. performed all in vivo studies, E.R.D. performed in vitro liver stage assays, U.R., V.P., A.K.L., S.E.B. assisted in vitro blood stage Plasmodium culture experiments, C.B.C. performed mass-spec analysis, H.Z. expressed and purified recombinant protein, performed biochemical assays, M.W. performed cytotoxicity assays, R.M. and S.A.S. Designed, synthesized and characterized small molecule inhibitors. J.D.H., L.R.H., G.E., K.G., V.Z., C.B.C., H.Z., P.S., S.L., M.M.M., O.W., D.F.W., R.M. analyzed data, W.J.S. contributed reagents, W.J.S., P.S., S.L., J.C., M.M.M., T.L.K., M.W., O.W., D.F.W., R.M. provided scientific leadership.

Competing interests: R.M. is consultant to Acetylon Pharmaceuticals and ERX Pharmaceuticals, and member on the advisory board of Malaria Free World; D.F.W. serves on the board of the Burroughs Wellcome Fund and the Marine Biological Lab; J.C. is consultant to Warp Drive Bio; S.L. is member on the Board of Directors of Johnson & Johnson and consultant to Yumanity; C.B.C. is consultant to Agios Pharmaceuticals, Capital Royalty, SynapDx Corp., General Metabolics. Following patent applications have been filed by Harvard University (PCT/US2008/61188740 and PCT/US2012/61586271)

Data and materials availability: The sequencing reads were deposited in National Center for Biotechnology Information (NCBI) Sequence Read Archive (SRA) (<http://www.ncbi.nlm.nih.gov/Traces/sra/>) under SRX110289 (HGFR-I) and SRX158283 (HGFR-II).

- ¹The Broad Institute, Infectious Diseases Initiative, Cambridge, MA 02142, USA
- ²Harvard School of Public Health, Department of Immunology and Infectious Disease, Boston, MA 02115, USA
- ³Biological and Biomedical Sciences, Boston, MA, USA
- ⁴Harvard/MIT Division of Health Sciences and Technology, Boston, MA, USA
- ⁵Harvard/MIT MD-PhD Program, Harvard Medical School, Boston, MA, USA
- ⁶Whitehead Institute for Biomedical Research, Cambridge, MA 02142, USA
- ⁷Department of Chemistry and Biochemistry, University of Notre Dame, Notre Dame, IN 46556, USA
- ⁸Center for Rare and Neglected Diseases, University of Notre Dame, Notre Dame, IN 46556, USA
- ⁹Instituto de Medicina Molecular, Faculdade de Medicina Universidade de Lisboa, 1649-028 Lisbon, Portugal
- ¹⁰Massachusetts General Hospital, Center for Systems Biology, Boston, MA 02114, USA
- ¹¹Instituto de Investigação do Medicamento (iMed.Ulisboa), Faculdade de Farmácia, Universidade de Lisboa, Av. Professor Gama Pinto, 1640-003, Lisbon, Portugal
- ¹²Harvard Medical School, Department of Biological Chemistry and Molecular Pharmacology, Boston, MA 02115, USA
- ¹³Department of Pharmacology and Toxicology and Microbiology and Immunology, Indiana University School of Medicine, Indianapolis, IN 46202, USA
- ¹⁴The Skaggs Institute for Chemical Biology, Department of Molecular Biology, The Scripps Research Institute, 10550 North Torrey Pines Road, La Jolla, California 92037, USA
- ¹⁵The Scripps Research Institute, Florida, 130 Scripps Way, Jupiter, FL 33458, USA
- ¹⁶Howard Hughes Medical Institute, Department of Biology, Massachusetts Institute of Technology, Cambridge, MA 02139, USA
- ¹⁷Department of Developmental Biology, Harvard School of Dental Medicine, Boston, MA 02115, USA
- ¹⁸School of Chemical Biology and Biotechnology, Laboratory for Computational Chemistry and Drug Design, Peking University, Shenzhen Graduate School, Shenzhen 518055, China

Abstract

The emergence of drug resistance is a major limitation of current antimalarials. The discovery of new druggable targets and pathways including those that are critical for multiple life cycle stages of the malaria parasite is a major goal for the development of the next-generation of antimalarial drugs. Using an integrated chemogenomics approach that combined drug-resistance selection, whole genome sequencing and an orthogonal yeast model, we demonstrate that the cytoplasmic prolyl-tRNA synthetase (*PfcPRS*) of the malaria parasite *Plasmodium falciparum* is a biochemical

and functional target of febrifugine and its synthetic derivatives such as halofuginone. Febrifugine is the active principle of a traditional Chinese herbal remedy for malaria. We show that treatment with febrifugine derivatives activated the amino acid starvation response in both *P. falciparum* and a transgenic yeast strain expressing *Pfc*PRS. We further demonstrate in the *P. berghei* mouse model of malaria that halofuginol, a new halofuginone analog that we developed, is highly active against both liver and asexual blood stages of the malaria parasite. Halofuginol, unlike halofuginone and febrifugine, is well tolerated at efficacious doses, and represents a promising lead for the development of dual-stage next generation antimalarials.

Introduction

Almost one-third of the world's population is exposed to malaria, with the highest burden of disease found in low-income nations in Asia, South America, and Africa. The World Health Organization (WHO) estimates that malaria parasites infect over 200 million people each year, killing approximately 600,000 people---mostly young children and pregnant women in sub-Saharan Africa---while many more suffer permanent disabilities (1).

The causative agents of malaria are protozoan parasites of the genus *Plasmodium* that are transmitted between human hosts by mosquitoes. In humans, parasites progress through a liver stage, an asexual symptomatic stage and a sexual blood stage. The emergence and spread of clinical resistance to mainstay drugs, including artemisinin and its derivatives, is the major limitation of current antimalarial drugs (2–4). Developing therapies that act on unexploited vulnerabilities in the *Plasmodium* parasite is necessary for renewed worldwide efforts to ultimately eradicate malaria (5). Thus, the discovery not only of new chemical classes of potential anti-malaria compounds, but also of new druggable targets and pathways is essential (6).

To address this need, we chose to target the prolyl-tRNA synthetase (PRS) of *P. falciparum* based on our previous work demonstrating that the natural product febrifugine and its synthetic derivative halofuginone (Fig. 1A) potently inhibit activity of the bifunctional glutamyl-prolyl-tRNA synthetase (EPRS) of mammalian cells (7). Aminoacyl-tRNA synthetases (aaRSs) are validated targets in several microorganisms and have more recently been proposed as attractive targets for chemotherapeutic intervention in malaria (8–14).

The natural product febrifugine constitutes the curative ingredient of an ancient Chinese herbal remedy that has been used for over 2000 years for the treatment of fevers and malaria (15–17). However, poor tolerability has precluded the clinical development of either febrifugine or its synthetic derivative halofuginone for the treatment of malaria (17). Thus, our aim was to elucidate the molecular basis of the anti-parasitic activity of febrifugine analogs and to identify derivatives with improved tolerability that could serve as a starting point for rational drug development.

We have previously identified EPRS as the target of febrifugine analogs in metazoans (7). However, the tRNA synthetase machinery differs greatly between humans and P. falciparum. In humans, EPRS is the only enzyme with PRS-activity and forms the central framework of a multi-subunit complex that is involved in a diverse number of biological processes in

addition to its canonical synthetase activity (18). In contrast, *P. falciparum* expresses two putative PRS enzymes, one that acts in the apicoplast (*PfaPRS*, PF3D7_0925300) and one that acts in the cytoplasm (*PfcPRS*, PF3D7_1213800) (19). Due to the difference in tRNA synthetase machinery and the large evolutionary distance between humans and *P. falciparum*, we selected an unbiased approach to identify the target of febrifugine derivatives in *P. falciparum*.

Here, we report the validation of *PfcPRS* as the functional target of febrifugine analogs. We identify halofuginol as a new halofuginone analog that may be a promising lead compound with potent *in vivo* efficacy against the liver and blood stages of the mouse malaria parasite *P. berghei*.

Results

The Cytoplasmic Prolyl-tRNA Synthetase of *P. falciparum* is a Molecular Target of Febrifugine and its Analogs

To identify the molecular target, we chose the select-seq experimental design in which we selected, *in vitro*, independent drug resistance *P. falciparum* parasites and sequenced the genomes to identify genetic mutations in *P. falciparum* associated with resistance to febrifugine and its analogs (20) (21). We carried out resistance selections in the wildtype Dd2 strain of *P. falciparum* exposed to halofuginone ($EC_{50} = 0.5$ nM) resulting in two highly resistant parasite lines that were independently selected: HFGR-I (halofuginone resistant line I; $EC_{50} = 180$ nM) and HFGR-II ($EC_{50} = 30$ nM) (Fig. 1B) (22). Both resistant strains were found to be cross-resistant to febrifugine (table S1).

To identify the genetic loci that contribute to halofuginone resistance we sequenced the full genome of the HFGR-I and HFGR-II *P. falciparum* strains along with the parental Dd2 strain (23, 24). The only gene with nonsynonymous single nucleotide polymorphisms (SNPs) identified in both resistant lines was PF3D7_1213800, which was annotated as a putative cytoplasmic proline amino acyl tRNA synthetase that resembled the *P. falciparum* PRS isoform with closest homology to the human orthologue (19). The independently selected mutations, T1445A and C1444T, occurred in the same codon of *PfcPRS* (Fig. 1C) translating into a L482H (HFGR-I) and L482F (HFGR-II) amino acid change. Both SNPs were independently confirmed by high resolution melting genotyping (fig. S1) and were verified by Sanger sequencing (25). None of the SNPs identified through our selection experiments corresponded to any of the 9 nonsynonymous SNPs in PF3D7_1213800 that are catalogued in PlasmoDB in naturally occurring *P. falciparum* strains (26). These data are consistent with our observation that halofuginone is equally active in a panel of 31 representative *P. falciparum* clinical isolates with diverse drug resistance profiles (fig. S2). These results suggest that *PfcPRS* may be the primary target of halofuginone and febrifugine. This possibility was further supported by the observation that addition of exogenous proline to the *in vitro* culture media of *P. falciparum* increased the IC₅₀ of halofuginone in a concentration dependent manner, although only ~3-fold shift in inhibition was observed following a 50-fold increase in proline concentration in the culture media (fig. S3).

Replacement of Yeast PRS by PfcPRS Confers Sensitivity to Halofuginone in Yeast

To validate *PfcPRS* as the functional target of halofuginone, we used a yeast transgenic system. The PRS of the yeast *Saccharomyces cerevisiae* (*ScPRS*, YHR020w) is similar to the *PfcPRS*. However, we discovered that *S. cerevisiae* was not sensitive to halofuginone. This allowed us to use yeast as an orthogonal model for both target confirmation of halofuginone and validation of the resistance phenotype of the mutant alleles identified in our drug resistance selections (fig. 2).

First, we performed a complementation test of *PfcPRS* in *S. cerevisiae*. We found that episomal expression of *PfcPRS* could complement deletion of the chromosomal copy of *ScPRS*, an essential gene and the only locus that encodes a PRS in *S. cerevisiae*. Next, we generated transgenic yeast strains that would episomally express only *ScPRS* or only *PfcPRS* (fig. 2A). Whereas both strains exhibited comparable growth characteristics, only the *PfcPRS*-expressing strain displayed a dose-dependent sensitivity to halofuginone treatment (fig. 2B, fig. S4), which was attenuated by addition of free L-proline (fig. S5).

To validate the resistance allele L482H, we also generated a yeast strain expressing L482H *PfcPRS* (fig. 2A). This strain was viable both in the presence and absence of halofuginone consistent with the L482H mutation conferring resistance to halofuginone (fig. 2B). Similar activity was observed for the L482F mutant, while none of the tested yeast strains were susceptible to inhibition by the control compound MAZ1310 (fig. 1A), a halofuginone analog that does not bind to PRS (7, 27). These results taken together confirmed that *PfcPRS* is the functional target of febrifugine and halofuginone and that mutation of amino acid 482 in *PfcPRS* conferred resistance to febrifugine and halofuginone.

Febrifugine and Halofuginone Induce the Amino Acid Starvation Response in *P. falciparum*

Following validation of *PfcPRS* as a molecular target of febrifugine and its analogs, we next investigated how halofuginol dysregulates the amino acid sensing mechanism in the parasite. In mammalian cells, inhibition of EPRS by halofuginone or direct amino acid deprivation results in phosphorylation of the eukaryotic initiation factor 2 α (eIF2 α) and consequent activation of the amino acid response (AAR) pathway (fig. S6) (7, 28). Recent research has confirmed the existence of a functional AAR in the intraerythrocytic stage of *P. falciparum* and has demonstrated induction of phosphorylated eIF2 α in response to amino acid starvation (13, 29).

To probe for the activation of the AAR, we treated asynchronous *P. falciparum* Dd2 cultures with halofuginone, febrifugine, or MAZ1310 as a negative control and quantified the amount of eIF2 α and phosphorylated eIF2 α by Western blot analysis compared to amino acid deprivation. Halofuginone and febrifugine treatment increased eIF2 α phosphorylation in a dose-dependent manner that was comparable to eIF2 α phosphorylation during amino acid starvation (fig. 2C, fig. S7). DMSO and MAZ1310 control treatments failed to increase eIF2 α phosphorylation.

Next, we investigated the effect of halofuginone treatment on eIF2 α phosphorylation in yeast strains expressing *PfcPRS* or *ScPRS*. Only the halofuginone-sensitive *PfcPRS*

expressing strain exhibited robust induction of phosphorylated eIF2 α in response to exposure to the compound (fig. 2D), whereas no difference in eIF2 α phosphorylation was observed in the *Sc*PRS expressing yeast strain. These results taken together demonstrate that halofuginone treatment induced the amino acid starvation pathway through direct inhibition of *Pfc*PRS.

Molecular Characterization of the Ligand-Target Interaction

To provide a structural rationale for the experimental results and to aid rational drug design efforts, we modeled the binding mode of the *Pfc*PRS to ATP and halofuginone based on the recently published structure of the ternary human PRS complex (PDB: 4HVC) (30). Our model showed that the N-protonated hydroxypiperidine moiety of halofuginone was stabilized by a network of hydrogen bond interactions (fig. 3A), which were not formed by MAZ1310. The interactions between halofuginone, ATP and *Pfc*PRS were similar to the binding mode observed for human PRS consistent with the similarity of the *Pfc*PRS core catalytic domains. These results show that halofuginone is a competitive inhibitor of the proline and tRNA binding sites of *Pfc*PRS (30).

Within the core class II catalytic domains, *Sc*PRS shares 77% and 70% similarity with human and *Plasmodium* enzymes, respectively (fig. S8). Comparison of *Pfc*PRS to *Sc*PRS provided insights into the unexpected differential activity of halofuginone in *P. falciparum* and *S. cerevisiae*. Even though the active site residues that interact with halofuginone were identical in both organisms, molecular dynamic simulations revealed the origin of the experimentally observed insensitivity of *S. cerevisiae* *Sc*PRS, which was not recognized by halofuginone in a standard docking approach. Unlike *Pfc*PRS, the geometry of the ternary *Sc*PRS-halofuginone-ATP complex was not stable, resulting in significant structural rearrangement of several amino acid side chains and the reorientation of the quinazoline moiety of halofuginone (compare Fig. 3A with Fig. 3B). We speculated that the structural change may be attributable to a threonine to serine mutation in position 512 (numbering based on *Pfc*PRS). T512 is conserved in the PRS of all halofuginone-sensitive apicomplexan parasites, and also in the EPRS of mouse and human. The presence of S512 in the yeast PRS resulted in a slightly altered binding mode for adenosine, which in turn impacted the halofuginone-ATP interaction and consequently altered the orientation of halofuginone (fig. 3B). The critical role of ATP for halofuginone binding is consistent with our previous finding that ATP is required for tight binding of halofuginone to human EPRS (7, 30). Furthermore, Hwang and Yogavel have recently solved the structures of free human EPRS and *Pfc*PRS, respectively, demonstrating significant conformational changes in the apo-enzyme (31, 32).

Next, we investigated the L482H *Pfc*PRS mutant to understand the experimentally observed decreased sensitivity of this mutant to halofuginone. L482 is adjacent to the proline-binding pocket and did not directly interact with either halofuginone or proline. However, our molecular dynamic simulations revealed that E361 moves from a position where it interacts with halofuginone (fig. 3C) to a position where it interacts with S508 and Y365. We hypothesized that this structural change was due to the hydrogen bond that the mutant H482 residue established with S508, thus re-orienting S508 such that it formed a hydrogen bond

with E361. The experimental observation that the L482H mutant is less strongly inhibited by halofuginone underscored the critical importance of this interaction. The L482F mutation observed in the other resistant parasite line in contrast induced steric repulsion with residues nearby, disrupting the interactions in the binding pocket (fig. S9). The results of our molecular dynamic simulations were consistent with the biological activity of halofuginone and established a detailed mechanistic explanation for the L482 resistance mutations and the unexpected insensitivity of *Sc*PRS, both of which were difficult to rationalize by standard molecular docking approaches.

Halofuginol is Active Against the Asexual Erythrocytic and Liver Stages of *P. falciparum* In Vitro

Dose-limiting toxicity, rather than lack of efficacy, has precluded clinical development of febrifugine and its analogs such as halofuginone as antimalarial drugs (17). We speculated that the observed side effects of halofuginone and febrifugine could, at least in part, be independent from inhibition of the human PRS. We proposed that the off-target effects may originate from the ability of the compounds to epimerize in solution through formation of a reactive intermediate enabled by the central ketone common to febrifugine and halofuginone (fig. S10) (33). Previously reported efforts to remove this functionality resulted in loss of activity (34). We reasoned that formal reduction of the ketone to yield a secondary alcohol would eliminate the ability to form a reactive Michael-acceptor, while retaining the functionality to form the critical hydrogen bonds within the target complex. Introduction of the alcohol also introduced an additional stereocenter. We therefore established synthetic approaches to access both epimers (fig. 4A). (7, 34)

Both compounds were tested for *in vitro* activity against the asexual blood stage of the *P. falciparum* 3D7 parasite strain. One epimer, halofuginol, demonstrated low nanomolar potency ($EC_{50} = 5.8$ nM) comparable to febrifugine ($EC_{50} = 4.0$ nM), whereas the other diastereomer, epi-halofuginol, was approximately 700-fold less active than halofuginone (Fig. 4B). As expected, the principle activity was attributable to one enantiomer, (2'S,2R,3S)-halofuginol, with the same absolute configuration of the piperidyl substituent as febrifugine and the active enantiomer of halofuginone (table S1). (35)

Cytotoxicity profiling in primary mouse embryonic fibroblasts ($EC_{50} = 373$ nM) revealed that halofuginol was approximately 65 times more selective for *P. falciparum*. Halofuginol had similar activity ($EC_{50} = 14$ nM) to halofuginone ($EC_{50} = 17$ nM) in the *in vitro* *P. berghei* ANKA liver stage model (fig. 4C) (36). As expected, the activity profile of halofuginol in the HFGR parasite lines and in the transgenic *Pfc*PRS yeast strains was comparable to that for halofuginone (fig. S11). In addition, treatment of *P. falciparum* with halofuginol *in vitro* resulted in the phosphorylation of eIF2 α in a similar manner to that observed with halofuginone (fig. S12A, B).

Furthermore, in biochemical studies, we demonstrated that the affinity of halofuginol for mutant *Pfc*PRS ($K_i = 1120 \pm 94.4$ nM) was approximately 16-fold less compared to the wildtype enzyme ($K_i = 71.1 \pm 9.0$ nM). In addition, we found that the L482H resistance mutation also resulted in a 6.4-fold decreased affinity for proline ($K_{m(wt)} = 117.0 \pm 11.2$ μ M and $K_{m(L482H)} = 747.7 \pm 36.5$ μ M). The biochemical characterization of human EPRS

revealed virtually identical affinities for halofuginol ($K_i = 65.7 \pm 6.3$ nM) and proline ($K_m = 135.4 \pm 9.8$ μ M) compared to wildtype *Pfc*PRS. These results, taken together, are consistent with our hypothesis that reduction of the central ketone to eliminate the undesired ability to form a reactive Michael-acceptor, while preserving the hydrogen bond acceptor capacity, would result in reduced cytotoxicity in mammalian cells while retaining on target activity in *Plasmodium* spp.

Halofuginol is Efficacious In Vivo

To further assess halofuginol in an *in vivo* system, we used an adapted version of Peters' suppressive test (37, 38) in a *P. berghei* mouse model of malaria. We found that halofuginol dosed daily at 12 mg/kg orally over 4 days reduced *P. berghei* parasite burden > 99% by day 5 relative to control untreated mice that had an average parasitemia of 8.9% (fig. 4D). Similar results were observed for i.p. administration of halofuginol at 12 mg/kg q.d. for 10 days (Fig. 4D). Both treatment strategies were very well tolerated and did not induce any adverse effects or gross pathological changes such as diarrhea, gastrointestinal hemorrhages/lesions, or discoloration of liver and spleen, which are the principle limiting toxicities observed with febrifugine and halofuginone treatment at efficacious doses (17). However, neither dosing strategy resulted in a sterilizing cure and parasites recrudesced after discontinuation of drug treatment.

We next investigated the *in vivo* activity of halofuginol in a *P. berghei* sporozoite challenge model (38). As shown in figure 5A, halofuginol reduced the load of liver stage parasites by >99% (at 46 hours post infection) following oral administration of a single 25 mg/kg dose, which we had established as a safe single dose treatment; treatment with 5 mg/kg i.p. or 10 mg/kg p.o. halofuginol reduced parasite burden by 99% and 95% , respectively (fig. 5B). Mice treated at 25 mg/kg p.o. were maintained for 14 days post infection or until they developed blood stage malaria. All mice in the control group developed blood stage malaria by day 4, whereas development of blood stage malaria was delayed in the treated group and 60% of the test animals were considered cured after 2 weeks (fig. 5C). Importantly, none of the treated animals displayed signs of adverse drug reactions (fig. S13). Separately, we tested halofuginone in the same *P. berghei* sporozoite challenge model and demonstrated that halofuginone is also efficacious in reducing liver stage infection (fig. S14). However, at efficacious doses, we observed pronounced gastrointestinal toxicities (4/5) and lethality (1/5), similar to reports evaluating halofuginone for *in vivo* blood stage activity (17). These results are consistent with the reduced cytotoxicity of halofuginol *in vitro* and support our hypothesis that chemical modification of the central ketone improves tolerability while retaining antimalarial activity *in vivo*.

Discussion

Developing therapies that act on unexploited vulnerabilities in the *Plasmodium* parasite will be necessary for renewed worldwide efforts to eradicate malaria (5). Febrifugine was identified over 60 years ago as the active principle of one of the oldest known antimalarial herbal remedies (16). However, poor tolerability prevented the clinical use of febrifugine as

a mainstay antimalarial and previous medicinal chemistry efforts failed to identify viable alternatives (17).

We set out to address two issues: First, the identification of the functional target of febrifugine and its derivatives in *P. falciparum* in order to facilitate rational drug development. Second, we sought to develop derivatives with reduced cytotoxicity in the human host.

Using an unbiased target identification approach, we report the identification and validation of *PfcPRS*, one of two prolyl-tRNA synthetases encoded in the *Plasmodium* genome and show that *PfcPRS* is the biochemical and functionally relevant target of febrifugine analogs. We support our findings by target validation in an orthogonal transgenic yeast model and provide a mechanistic rationale for drug action at a molecular level. We established that halofuginol, a new halofuginone analog previously developed by our group, had excellent *in vivo* activity in two *P. berghei* malaria mouse models against the liver stage and the asexual blood stage of the parasite. Dual-stage activity is essential for antimalarial drugs that will be used to eliminate malaria. However, *in vivo* activity against the liver stage of the malaria parasite by febrifugine derivatives has not been demonstrated before. Notably, we were able to show that a single oral dose of 25 mg/kg halofuginol resulted in >99% reduction in liver parasites and an overall 60% cure-rate in the *P. berghei* liver stage model. Halofuginol was also highly efficacious against the asexual blood stage as demonstrated by >99% reduction in parasitemia following a 4-day oral treatment at 12 mg/kg, but failed to result in a sterile cure. Importantly, at pharmaceutically efficacious concentrations, halofuginol was better tolerated than febrifugine and halofuginone and did not induce any adverse effects even after daily i.p. administration at 12 mg/kg for 10 days.

Previous reports have suggested that tRNA synthetases represent attractive targets for the treatment of malaria (8–13, 39). Recently, Winzeler and coworkers identified cladosporin, a fungal metabolite previously not known to have inhibitory activity against amino acyl tRNA synthetase, as a selective and specific inhibitor of the *P. falciparum* lysyl-tRNA synthetase with mid-nanomolar *in vitro* activity against blood and liver-stage parasites (14). In addition, the isoleucyl tRNA synthetase (IRS) inhibitors mupirocin and the isoleucine analog thiaisoleucine have been shown to target the apicoplast IRS and cytoplasmic IRS, respectively, and can kill blood stage parasites at mid-nanomolar and low micromolar concentrations (13). However, thiaisoleucine did not induce eIF2 α phosphorylation, which is a sensitive indicator of the starvation response and a hallmark of isoleucine withdrawal, suggesting that the antiparasitic activity of thiaisoleucine is due to inhibition of secondary targets (13). An alternative explanation is that this could be the result of insufficient inhibition of IRS activity at the tested concentrations due to the short half-life or low potency of the compound.

In contrast, we show that febrifugine analogs induce eIF2 α phosphorylation in *Plasmodium* parasites and transgenic yeast expressing *PfcPRS*. This establishes a valuable chemical tool with which to study the amino acid starvation pathway in *P. falciparum* and *S. cerevisiae*, and also validates *PfcPRS* as an attractive target for the development of new classes of antimalarials that are active against both the erythrocytic and liver stages of the malaria

parasite. Additionally, the transgenic yeast strain reported here in combination with halofuginone could prove valuable for mechanistically dissecting nutrient deprivation signaling pathways in eukaryotes and to study the independence and interrelatedness of nutrient sensing by the AAR and the TOR pathways (40).

We speculate that the broad-spectrum antiprotozoal activity of halofuginone could be due to conservation of PRS. Halofuginone is currently approved in veterinary medicine to treat coccidiosis in poultry (caused by *Eimeria tenella*) and cryptosporidiosis in cattle (caused by *Cryptosporidium parvum*) (41–43). Molecular phylogenetics of the catalytic domain confirms that *E. tenella* PRS and *C. parvum* PRS share 81% and 86% similarity with *PfcPRS*, respectively (fig. S7). Furthermore, these agents may be effective against other human malaria parasites such as *P. vivax*, which shares 95% conservation of the active site of the *PfcPRS*, and a wide swath of infectious diseases caused by protozoan parasites including toxoplasmosis, babesiosis and Chaga's disease.

The ability to generate and isolate *P. falciparum* lines that are genetically resistant to halofuginone was critical to our approach to identify and validate *PfcPRS* as a target for malaria drug development. However, as is true for any antimalarial drug, resistance also constitutes a concern for potential clinical use of *PfcPRS* inhibitors. Although our studies did not investigate the long-term stability and fitness costs of the identified resistance mutations in *P. falciparum* in the context of competing wildtype parasites, we are encouraged that all identified mutations in *PfcPRS* mapped to the same amino acid codon, which suggests that mutational plasticity could be restricted for this target. Nonetheless, additional research is needed to investigate this issue in greater detail. In this context, it will also be of interest to identify drug combinations that synergize with *PfcPRS* inhibitors.

Although our studies identify halofuginol as an attractive starting point for rational development of *PfcPRS* inhibitors as next-generation antimalarials, detailed drug metabolism and pharmacokinetics studies will be needed to better understand the *in vivo* pharmacology of this compound and to guide future drug development. In particular, it will be important to understand the consequences of blocking human EPRS. *PfcPRS* inhibitors with improved biochemical selectivity might be more attractive candidates for clinical development. Our next goal will be to focus on the development of such compounds. Combined with our recent identification of the human EPRS as the target of halofuginone, the computational and mechanistic studies presented here provide a detailed understanding of the ligand-protein interaction at atomic resolution in both the human and parasite enzymes, establishing a clear path forward to the design of new inhibitors with dual-stage activity that selectively target the malaria parasite.

Materials and Methods

Study Design

The objective of this study was to identify and validate the target of febrifugine and its derivatives in *Plasmodium falciparum* and to assess their *in vivo* efficacy and tolerability in mouse models of liver and blood stage malaria. First, two halofuginone resistant lines were independently selected under intermittent drug pressure and sequenced. Whole-genome

analysis identified the cytoplasmic prolyl tRNA synthetase (*PfcPRS*, PF3D7_1213800) as the only gene with mutations in both strains. Next, *PfcPRS* was validated as a mechanistic target in a transgenic yeast system by replacing the halofuginone-insensitive yeast homolog *ScPRS* with wild-type and mutant *PfcPRS*, which yielded halofuginone-sensitive and halofuginone-insensitive strains, respectively. Separately, wild-type and mutant *PfcPRS* were purified and biochemically characterized to confirm *PfcPRS* as a molecular target of halofuginone analogs, and functional validation led to identification of resistance mutations. In addition molecular dynamic simulations were performed to provide a mechanistic rationale for the identified resistance mutations and the lack of affinity of halofuginone for yeast PRS. All *in vitro* experiments were repeated at least twice. Finally, halofuginone and the modified analog halofuginol were evaluated in mice for efficacy against liver and blood stage malaria. Mice were infected and randomized into different groups before drug treatment. Investigators were not blinded for animal allocation, compound administration, clinical evaluation of mice, or during the evaluation of collected tissues.

All *in vivo* protocols were approved by the Animal Care Committee of the Instituto de Medicina Molecular, University of Lisbon; and were performed according to the regulations of the European guidelines 86/609/EEG. Guidelines for humane endpoints were strictly followed for all *in vivo* experiments.

Statistical analysis

Statistical analyses were performed in Prism 6.0 (GraphPad Software Inc.). Data are shown as means \pm SD. Analytical tests for statistical significance and P values are specified in each figure legend. EC₅₀ values were calculated using a four-parameter nonlinear regression curve fit. Ordinary one-way ANOVA (Sidak's multiple comparison test) was used for comparison of 3 or more groups. Mann-Whitney test was used for two groups. For survival data, the Kaplan-Meier method and log-rank (Mantel-Cox test) was used for comparisons between groups.

Supplementary Material

Refer to Web version on PubMed Central for supplementary material.

Acknowledgments

We would like to acknowledge Rachel Daniels for advice on assay design and experimental guidance.

Funding: We gratefully acknowledge financial support from the Gates Foundation (DFW and RM OPP1086203), the National Institute of Health (DFW) AI105786 (WJS), 5F32AI084440-02 (LRP), CA92577 (PS), GM099796 (ERD), The Center for Rare and Neglected Diseases at the University of Notre Dame (OW, GE), generous allocation of computing resources by the National Science Foundation through TeraGrid grant TG-CHE090124 (OW), A fellowship from the National Foundation for Cancer Research (PS), SFRH/BD/80162/2011 (SAS), PTDC/SAU-MIC/113697/2009 (VZL) and EXCL/IMI-MIC/0056/2012 (MMM) (Fundação para a Ciência e Tecnologia, Portugal), Howard Hughes Medical Institute (SL) and start-up funding provided by the Center for Systems Biology/Mass. General Hospital (RM).

References

1. World Health Organization. World health statistics 2012. World Health Organization; 2012.

2. Arie F, Witkowski B, Amaratunga C, Beghain J, Langlois AC, Khim N, Kim S, Duru V, Bouchier C, Ma L, Lim P, Leang R, Duong S, Sreng S, Suon S, Chuor CM, Bout DM, Menard S, Rogers WO, Genton B, Fandeur T, Miotto O, Ringwald P, Le Bras J, Berry A, Barale JC, Fairhurst RM, Benoit-Vical F, Mercereau-Puijalon O, Menard D. A molecular marker of artemisinin-resistant *Plasmodium falciparum* malaria. *Nature*. 2014; 505:50–55. [PubMed: 24352242]
3. Wongsrichanalai C, Meshnick SR. Declining artesunate-mefloquine efficacy against falciparum malaria on the Cambodia-Thailand border. *Emerg. Infect. Dis.* 2008; 14:716–719. [PubMed: 18439351]
4. Fidock DA, Rosenthal PJ, Croft SL, Brun R, Nwaka S. Antimalarial drug discovery: efficacy models for compound screening. *Nat. Rev. Drug Discovery*. 2004; 3:509–520. [PubMed: 15173840]
5. Alonso PL, Brown G, Arevalo-Herrera M, Binka F, Chitnis C, Collins F, Doumbo OK, Greenwood B, Hall BF, Levine MM, Mendis K, Newman RD, Plowe CV, Rodriguez MH, Sinden R, Slutsker L, Tanner M. A research agenda to underpin malaria eradication. *PLoS Med*. 2011; 8:e1000406. [PubMed: 21311579]
6. Nilsen A, LaCrue AN, White KL, Forquer IP, Cross RM, Marfurt J, Mather MW, Delves MJ, Shackleford DM, Saenz FE, Morrisey JM, Steuten J, Mutka T, Li Y, Wirjanata G, Ryan E, Duffy S, Kelly JX, Sebayang BF, Zeeman AM, Noviyanti R, Sinden RE, Kocken CH, Price RN, Avery VM, Angulo-Barturen I, Jimenez-Diaz MB, Ferrer S, Herreros E, Sanz LM, Gamo FJ, Bathurst I, Burrows JN, Siegl P, Guy RK, Winter RW, Vaidya AB, Charman SA, Kyle DE, Manetsch R, Riscoe MK. Quinolone-3-diarylethers: a new class of antimalarial drug. *Sci. Transl. Med.* 2013; 5 177ra37.
7. Keller TL, Zocco D, Sundrud MS, Hendrick M, Edenius M, Yum J, Kim Y-J, Lee H-K, Cortese JF, Wirth DF, Dignam JD, Rao A, Yeo C-Y, Mazitschek R, Whitman M. Halofuginone and other febrifugine derivatives inhibit prolyl-tRNA synthetase. *Nat. Chem. Biol.* 2012; 8:311–317. [PubMed: 22327401]
8. Pham JS, Sakaguchi R, Yeoh LM, De Silva NS, McFadden GI, Hou YM, Ralph SA. A dual-targeted aminoacyl-tRNA synthetase in *Plasmodium falciparum* charges cytosolic and apicoplast tRNACys. *Biochem. J.* 2014; 458:513–523. [PubMed: 24428730]
9. Jackson KE, Habib S, Frugier M, Hoen R, Khan S, Pham JS, Ribas de Pouplana L, Royo M, Santos MA, Sharma A, Ralph SA. Protein translation in *Plasmodium* parasites. *Trends Parasitol.* 2011; 27:467–476. [PubMed: 21741312]
10. Khan S, Sharma A, Jamwal A, Sharma V, Pole AK, Thakur KK, Sharma A. Uneven spread of cis- and trans-editing aminoacyl-tRNA synthetase domains within translational compartments of *P. falciparum*. *Sci. Rep.* 2011; 1:188. [PubMed: 22355703]
11. Zhang YK, Plattner JJ, Freund YR, Easom EE, Zhou Y, Ye L, Zhou H, Waterson D, Gamo FJ, Sanz LM, Ge M, Li Z, Li L, Wang H, Cui H. Benzoxaborole antimalarial agents. Part 2: Discovery of fluoro-substituted 7-(2-carboxyethyl)-1,3-dihydro-1-hydroxy-2,1-benzoxaboroles. *Bioorg. Med. Chem. Lett.* 2012; 22:1299–1307. [PubMed: 22243961]
12. Jackson KE, Pham JS, Kwek M, De Silva NS, Allen SM, Goodman CD, McFadden GI, de Pouplana LR, Ralph SA. Dual targeting of aminoacyl-tRNA synthetases to the apicoplast and cytosol in *Plasmodium falciparum*. *Int. J. Parasitol.* 2012; 42:177–186. [PubMed: 2222968]
13. Istvan ES, Dharia NV, Bopp SE, Gluzman I, Winzeler EA, Goldberg DE. Validation of isoleucine utilization targets in *Plasmodium falciparum*. *Proc. Natl. Acad. Sci. U S A.* 2011; 108:1627–1632. [PubMed: 21205898]
14. Hoepfner D, McNamara CW, Lim CS, Studer C, Riedl R, Aust T, McCormack SL, Plouffe DM, Meister S, Schuierer S, Plikat U, Hartmann N, Staedtler F, Costesta S, Schmitt EK, Petersen F, Supek F, Glynne RJ, Tallarico JA, Porter JA, Fishman MC, Bodenreider C, Diagana TT, Movva NR, Winzeler EA. Selective and Specific Inhibition of the *Plasmodium falciparum* Lysyl-tRNA Synthetase by the Fungal Secondary Metabolite Cladosporin. *Cell Host and Microbe.* 2012; 11:654–663. [PubMed: 22704625]
15. Tonkin IM, Work TS. A new anti-malarial drug. *Nature.* 1945; 156:630. [PubMed: 21006487]
16. Burns WR. East meets West: how China almost cured malaria. *Endeavour.* 2008; 32:101–106. [PubMed: 18691761]

17. Jiang S, Zeng Q, Gettayacamin M, Tungtaeng A, Wannaying S, Lim A, Hansukjariya P, Okunji CO, Zhu S, Fang D. Antimalarial activities and therapeutic properties of febrifugine analogs. *Antimicrob. Agents Chemother.* 2005; 49:1169–1176. [PubMed: 15728920]
18. Guo M, Schimmel P. Essential nontranslational functions of tRNA synthetases. *Nat. Chem. Biol.* 2013; 9:145–153. [PubMed: 23416400]
19. Bhatt TK, Kapil C, Khan S, Jairajpuri MA, Sharma V, Santoni D, Silvestrini F, Pizzi E, Sharma A. A genomic glimpse of aminoacyl-tRNA synthetases in malaria parasite *Plasmodium falciparum*. *BMC Genomics.* 2009; 10:644. [PubMed: 20042123]
20. Park DJ, Lukens AK, Neafsey DE, Schaffner SF, Chang HH, Valim C, Ribacke U, Van Tyne D, Galinsky K, Galligan M, Becker JS, Ndiaye D, Mboup S, Wiegand RC, Hartl DL, Sabeti PC, Wirth DF, Volkman SK. Sequence-based association and selection scans identify drug resistance loci in the *Plasmodium falciparum* malaria parasite. *Proc. Natl. Acad. Sci. U S A.* 2012; 109:13052–13057. [PubMed: 22826220]
21. Flannery EL, Fidock DA, Winzeler EA. Using Genetic Methods To Define the Targets of Compounds with Antimalarial Activity. *J. Med. Chem.* 2013; 56:7761–7771. [PubMed: 23927658]
22. Dong CK, Uргаonkar S, Cortese JF, Gamo F-J, Garcia-Bustos JF, Lafuente M, Patel V, Ross L, Coleman BI, Derbyshire E, Clish CB, Serrano AE, Cromwell M, Barker RH, Dvorin JD, Duraisingh MT, Wirth DF, Clardy J, Mazitschek R. Identification and Validation of Tetracycline Benzothiazepines as *Plasmodium falciparum* Cytochrome bc(1) Inhibitors. *Chem. Biol.* 2011; 18:1602–1610. [PubMed: 22195562]
23. Li H, Handsaker B, Wysoker A, Fennell T, Ruan J, Homer N, Marth G, Abecasis G, Durbin R, Subgroup GPP. The Sequence Alignment/Map format and SAMtools. *Bioinformatics (Oxford, England).* 2009; 25:2078–2079.
24. McKenna A, Hanna M, Banks E, Sivachenko A, Cibulskis K, Kernytzky A, Garimella K, Altshuler D, Gabriel S, Daly M, DePristo MA. The Genome Analysis Toolkit: a MapReduce framework for analyzing next-generation DNA sequencing data. *Genome Res.* 2010; 20:1297–1303. [PubMed: 20644199]
25. Daniels R, Ndiaye D, Wall M, McKinney J, Sene PD, Sabeti PC, Volkman SK, Mboup S, Wirth DF. Rapid, field-deployable method for genotyping and discovery of single-nucleotide polymorphisms associated with drug resistance in *Plasmodium falciparum*. *Antimicrob. Agents Chemother.* 2012; 56:2976–2986. [PubMed: 22430961]
26. Aurrecochea C, Brestelli J, Brunk BP, Dommer J, Fischer S, Gajria B, Gao X, Gingle A, Grant G, Harb OS, Heiges M, Innamorato F, Iodice J, Kissinger JC, Kraemer E, Li W, Miller JA, Nayak V, Pennington C, Pinney DF, Roos DS, Ross C, Stoeckert CJJ, Treatman C, Wang H. PlasmoDB: a functional genomic database for malaria parasites. *Nucleic Acids Res.* 2009; 37:D539–D543. [PubMed: 18957442]
27. Sundrud MS, Koralov SB, Feuerer M, Calado DP, Kozhaya AE, Rhule-Smith A, Lefebvre RE, Unutmaz D, Mazitschek R, Waldner H, Whitman M, Keller T, Rao A. Halofuginone inhibits TH17 cell differentiation by activating the amino acid starvation response. *Science.* 2009; 324:1334–1338. [PubMed: 19498172]
28. Hinnebusch AG. Translational regulation of GCN4 and the general amino acid control of yeast. *Annu. Rev. Microbiol.* 2005; 59:407–450. [PubMed: 16153175]
29. Fennell C, Babbitt S, Russo I, Wilkes J, Ranford-Cartwright L, Goldberg DE, Doerig C. PfeIK1, a eukaryotic initiation factor 2alpha kinase of the human malaria parasite *Plasmodium falciparum*, regulates stress-response to amino-acid starvation. *Malar. J.* 2009; 8:99. [PubMed: 19435497]
30. Zhou H, Sun L, Yang XL, Schimmel P. ATP-directed capture of bioactive herbal-based medicine on human tRNA synthetase. *Nature.* 2013; 494:121–124. [PubMed: 23263184]
31. Jain V, Kikuchi H, Oshima Y, Sharma A, Yogavel M. Structural and functional analysis of the anti-malarial drug target prolyl-tRNA synthetase. *J. Struct. Funct. Genomics.* 2014; 15:181–190. [PubMed: 25047712]
32. Son J, Lee EH, Park M, Kim JH, Kim J, Kim S, Jeon YH, Hwang KY. Conformational changes in human prolyl-tRNA synthetase upon binding of the substrates proline and ATP and the inhibitor halofuginone. *Acta Crystallogr. D Biol. Crystallogr.* 2013; 69:2136–2145. [PubMed: 24100331]

33. Takeuchi Y, Oshige M, Azuma K, Abe H, Harayama T. Concise synthesis of dl-febrifugine. *Chem. Pharm. Bull. (Tokyo)*. 2005; 53:868–869. [PubMed: 15997158]
34. Kikuchi H, Tasaka H, Hirai S, Takaya Y, Iwabuchi Y, Ooi H, Hatakeyama S, Kim HS, Wataya Y, Oshima Y. Potent antimalarial febrifugine analogues against the plasmodium malaria parasite. *J. Med. Chem.* 2002; 45:2563–2570. [PubMed: 12036365]
35. Linder MR, Heckerroth AR, Najdrowski M, Dausgschies A, Schollmeyer D, Miculka C. (2R,3S)-(+)- and (2S,3R)-(-)-Halofuginone lactate: synthesis, absolute configuration, and activity against *Cryptosporidium parvum*. *Bioorg. Med. Chem. Lett.* 2007; 17:4140–4143. [PubMed: 17544270]
36. Derbyshire ER, Mazitschek R, Clardy J. Characterization of Plasmodium liver stage inhibition by halofuginone. *ChemMedChem.* 2012; 7:844–849. [PubMed: 22438279]
37. Peters W. The chemotherapy of rodent malaria, XXII. The value of drug-resistant strains of *P. berghei* in screening for blood schizontocidal activity. *Ann Trop Med Parasitol.* 1975; 69:155–171. [PubMed: 1098584]
38. Hanson KK, Ressurreicao AS, Buchholz K, Prudencio M, Herman-Ornelas JD, Rebelo M, Beatty WL, Wirth DF, Hanscheid T, Moreira R, Marti M, Mota MM. Torins are potent antimalarials that block replenishment of Plasmodium liver stage parasitophorous vacuole membrane proteins. *Proc. Natl. Acad. Sci. U S A.* 2013; 110:E2838–E2847. [PubMed: 23836641]
39. Flannery EL, Chatterjee AK, Winzeler EA. Antimalarial drug discovery -approaches and progress towards new medicines. *Nat. Rev. Microbiol.* 2013; 11:849–862. [PubMed: 24217412]
40. Valbuena N, Rozalen AE, Moreno S. Fission yeast TORC1 prevents eIF2alpha phosphorylation in response to nitrogen and amino acids via Gcn2 kinase. *J. Cell Sci.* 2012; 125:5955–5959. [PubMed: 23108671]
41. Trotz-Williams LA, Jarvie BD, Peregrine AS, Duffield TF, Leslie KE. Efficacy of halofuginone lactate in the prevention of cryptosporidiosis in dairy calves. *Vet. Rec.* 2011; 168:509. [PubMed: 21546409]
42. Naciri M, Mancassola R, Yvove P, Peeters JE. The effect of halofuginone lactate on experimental *Cryptosporidium parvum* infections in calves. *Vet. Parasitol.* 1993; 45:199–207. [PubMed: 8447063]
43. Zhang DF, Sun BB, Yue YY, Yu HJ, Zhang HL, Zhou QJ, Du AF. Anticoccidial effect of halofuginone hydrobromide against *Eimeria tenella* with associated histology. *Parasitol. Res.* 2012; 111:695–701. [PubMed: 22415441]
44. Trager W, Jensen JB. Human malaria parasites in continuous culture. *Science.* 1976; 193:673–675. [PubMed: 781840]
45. Smilkstein M, Sriwilaijaroen N, Kelly JX, Wilairat P, Riscoe M. Simple and inexpensive fluorescence-based technique for high-throughput antimalarial drug screening. *Antimicrob. Agents Chemother.* 2004; 48:1803–1806. [PubMed: 15105138]
46. Bennett TN, Paguio M, Gligorijevic B, Seudieu C, Kosar AD, Davidson E, Roepe PD. Novel, rapid, and inexpensive cell-based quantification of antimalarial drug efficacy. *Antimicrob. Agents Chemother.* 2004; 48:1807–1810. [PubMed: 15105139]
47. Rosario V. Cloning of naturally occurring mixed infections of malaria parasites. *Science.* 1981; 212:1037–1038. [PubMed: 7015505]
48. Narasimhan J, Joyce BR, Naguleswaran A, Smith AT, Livingston MR, Dixon SE, Coppens I, Wek RC, Sullivan WJ. Translation regulation by eukaryotic initiation factor-2 kinases in the development of latent cysts in *Toxoplasma gondii*. *J. Biol. Chem.* 2008; 283:16591–16601. [PubMed: 18420584]
49. Hu Y, Rolfs A, Bhullar B, Murthy TVS, Zhu C, Berger MF, Camargo AA, Kelley F, McCarron S, Jepson D, Richardson A, Raphael J, Moreira D, Taycher E, Zuo D, Mohr S, Kane MF, Williamson J, Simpson A, Bulyk ML, Harlow E, Marsischky G, Kolodner RD, LaBaer J. Approaching a complete repository of sequence-verified protein-encoding clones for *Saccharomyces cerevisiae*. *Genome Res.* 2007; 17:536–543. [PubMed: 17322287]
50. Alberti S, Gitler AD, Lindquist S. A suite of Gateway cloning vectors for high-throughput genetic analysis in *Saccharomyces cerevisiae*. *Yeast (Chichester, England)*. 2007; 24:913–919.
51. Gietz RD, Woods RA. Transformation of yeast by lithium acetate/single-stranded carrier DNA/polyethylene glycol method. *Methods Enzymol.* 2002; 350:87–96. [PubMed: 12073338]

52. Ausubel, FM.; Brent, R.; Kingston, RE.; Moore, D.; Seidman, JG.; Struhl, K. *Current Protocols in Molecular Biology*. John Wiley & Sons, Incorporated; 2004. p. 1600
53. Gueldener U, Heinisch J, Koehler GJ, Voss D, Hegemann JH. A second set of loxP marker cassettes for Cre-mediated multiple gene knockouts in budding yeast. *Nucleic Acids Res.* 2002; 30:e23. [PubMed: 11884642]
54. Goldstein AL, McCusker JH. Three new dominant drug resistance cassettes for gene disruption in *Saccharomyces cerevisiae*. *Yeast (Chichester, England)*. 1999; 15:1541–1553.
55. Ploemen IH, Prudencio M, Douradinha BG, Ramesar J, Fonager J, van Gemert GJ, Luty AJ, Hermesen CC, Sauerwein RW, Baptista FG, Mota MM, Waters AP, Que I, Lowik CW, Khan SM, Janse CJ, Franke-Fayard BM. Visualisation and quantitative analysis of the rodent malaria liver stage by real time imaging. *PLoS ONE*. 2009; 4:e7881. [PubMed: 19924309]
56. Jacobson MP, Pincus DL, Rapp CS, Day TJ, Honig B, Shaw DE, Friesner RA. A hierarchical approach to all-atom protein loop prediction. *Proteins*. 2004; 55:351–367. [PubMed: 15048827]
57. Friesner RA, Murphy RB, Repasky MP, Frye LL, Greenwood JR, Halgren TA, Sanschagrin PC, Mainz DT. Extra precision glide: docking and scoring incorporating a model of hydrophobic enclosure for protein-ligand complexes. *J. Med. Chem.* 2006; 49:6177–6196. [PubMed: 17034125]
58. Friesner RA, Banks JL, Murphy RB, Halgren TA, Klicic JJ, Mainz DT, Repasky MP, Knoll EH, Shelley M, Perry JK, Shaw DE, Francis P, Shenkin PS. Glide: a new approach for rapid, accurate docking and scoring. 1. Method and assessment of docking accuracy. *J. Med. Chem.* 2004; 47:1739–1749. [PubMed: 15027865]
59. Estiu G, West N, Mazitschek R, Greenberg E, Bradner JE, Wiest O. On the inhibition of histone deacetylase 8. *Bioorg. Med. Chem.* 2010; 18:4103–4110. [PubMed: 20472442]
60. Case, DA.; Darden, TA.; Cheatham Iii, TE.; Simmerling, CL.; Wang, J.; Duke, RE.; Luo, R.; Crowley, M.; Walker, RC.; Zhang, W. *AMBER 10*. San Francisco: University of California; 2008.
61. Jorgensen WL, Chandrasekhar J, Madura JD, Impey RW, Klein ML. Comparison of simple potential functions for simulating liquid water. *J. Chem. Phys.* 1983; 79:926.
62. Schafmeister C, Ross WS, Romanovski V. *LEaP*. 1995
63. Wang J, Wolf RM, Caldwell JW, Kollman PA, Case DA. Development and testing of a general amber force field. *J. Comput. Chem.* 2004; 25:1157–1174. [PubMed: 15116359]
64. Wang J, Wang W, Kollman PA, Case DA. Automatic atom type and bond type perception in molecular mechanical calculations. *J. Mol. Graphics Modell.* 2006; 25:247–260.
65. Fox T, Kollman PA. Application of the RESP Methodology in the Parametrization of Organic Solvents. *J. Phys. Chem. B.* 2011; 102:8070–8079.
66. Ryckaert J-P, Ciccotti G, Berendsen HJC. Numerical integration of the cartesian equations of motion of a system with constraints: molecular dynamics of n-alkanes. *J. Comput. Phys.* 1977; 23:327–341.
67. Pastor R, Brooks B, Szabo A. An analysis of the accuracy of Langevin and molecular dynamics algorithms. *Mol. Phys.* 1988; 65:1409–1419.
68. Essmann U, Perera L, Berkowitz ML, Darden T, Lee H, Pedersen LG. A smooth particle mesh Ewald method. *J. Chem. Phys.* 1995; 103:8577.
69. Petersen HG. Accuracy and efficiency of the particle mesh Ewald method. *J. Chem. Phys.* 1995; 103:3668.
70. Marchler-Bauer A, Lu S, Anderson JB, Chitsaz F, Derbyshire MK, DeWeese-Scott C, Fong JH, Geer LY, Geer RC, Gonzales NR, Gwadz M, Hurwitz DI, Jackson JD, Ke Z, Lanczycki CJ, Lu F, Marchler GH, Mullokandov M, Omelchenko MV, Robertson CL, Song JS, Thanki N, Yamashita RA, Zhang D, Zhang N, Zheng C, Bryant SH. CDD: a Conserved Domain Database for the functional annotation of proteins. *Nucleic Acids Res.* 2011; 39:D225–D229. [PubMed: 21109532]

Accessible Summary

Malaria is a devastating disease. It is caused by a unicellular parasite and claims more than 600,000 lives every year - mostly young children and pregnant women. Renewed worldwide efforts to eradicate malaria demand novel therapeutic approaches to overcome the emergence and spread of clinical resistance to mainstay drugs.

We here validated the *Plasmodium* cytoplasmic prolyl-tRNA synthetase as the enigmatic target of the natural product febrifugine, the active principle of an herbal malaria remedy that has been used for millennia in Traditional Chinese Medicine, and establish a path forward to the rational development of next generation antimalaria therapies.

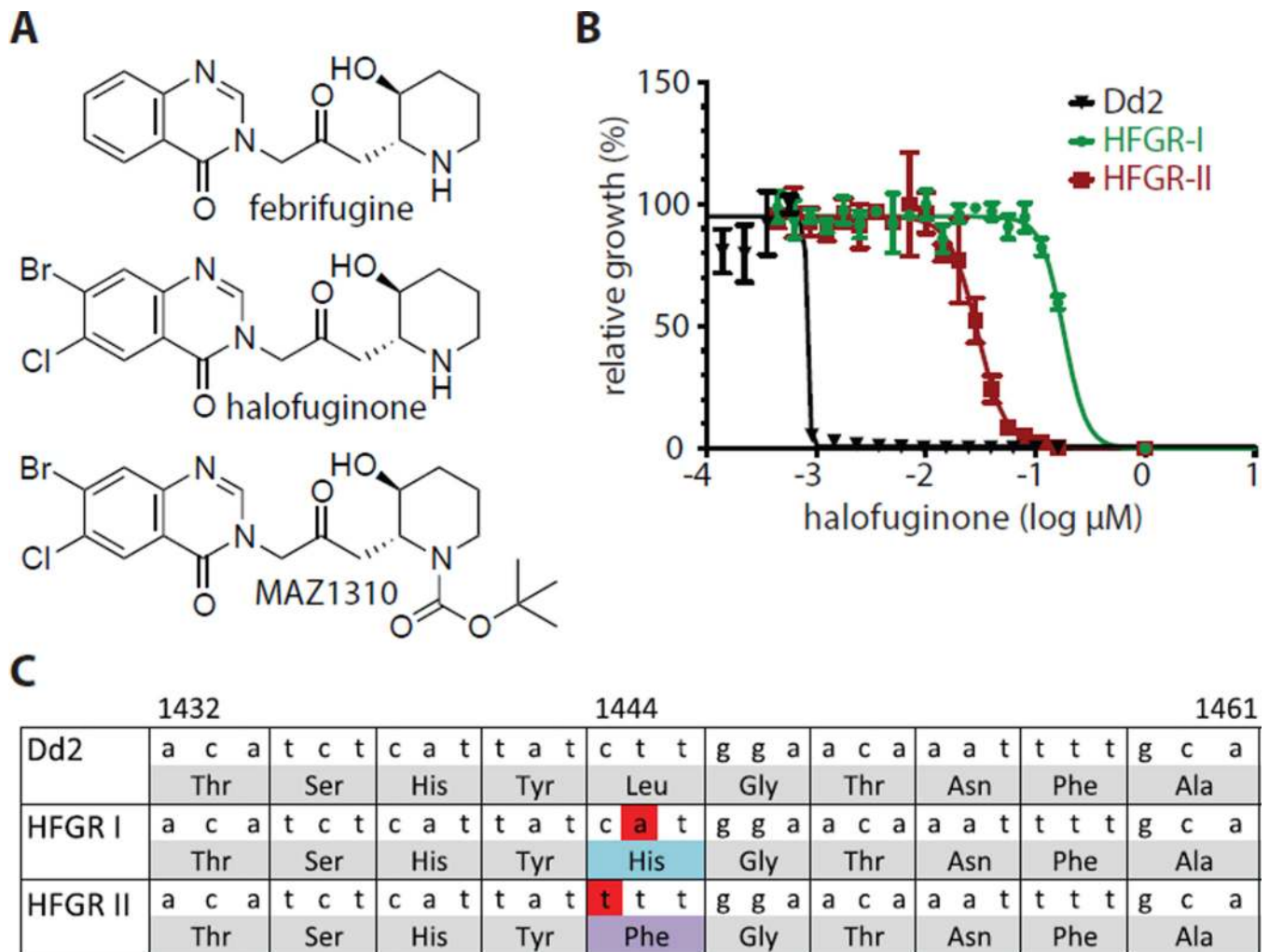


Figure 1. Identification and confirmation of *Pfc* PRS of *P. falciparum* as a target of halofuginone (A) Shown are chemical structures for febrifugine and its analogs halofuginone (relative stereochemistry) and MAZ1310 (relative stereochemistry). (B) Independent selection experiments under intermittent and dose-adjusted drug pressure starting with the Dd2 lab strain of *P. falciparum* yielded two highly resistant clones (HFGR-I and HFGR-II). (C) Whole genome sequencing identified nonsynonymous mutations in the highly resistant clones HFGR-I and HFGR-II that map to the same amino acid codon, L482, in *Pfc*PRS (PF3D7_1213800).

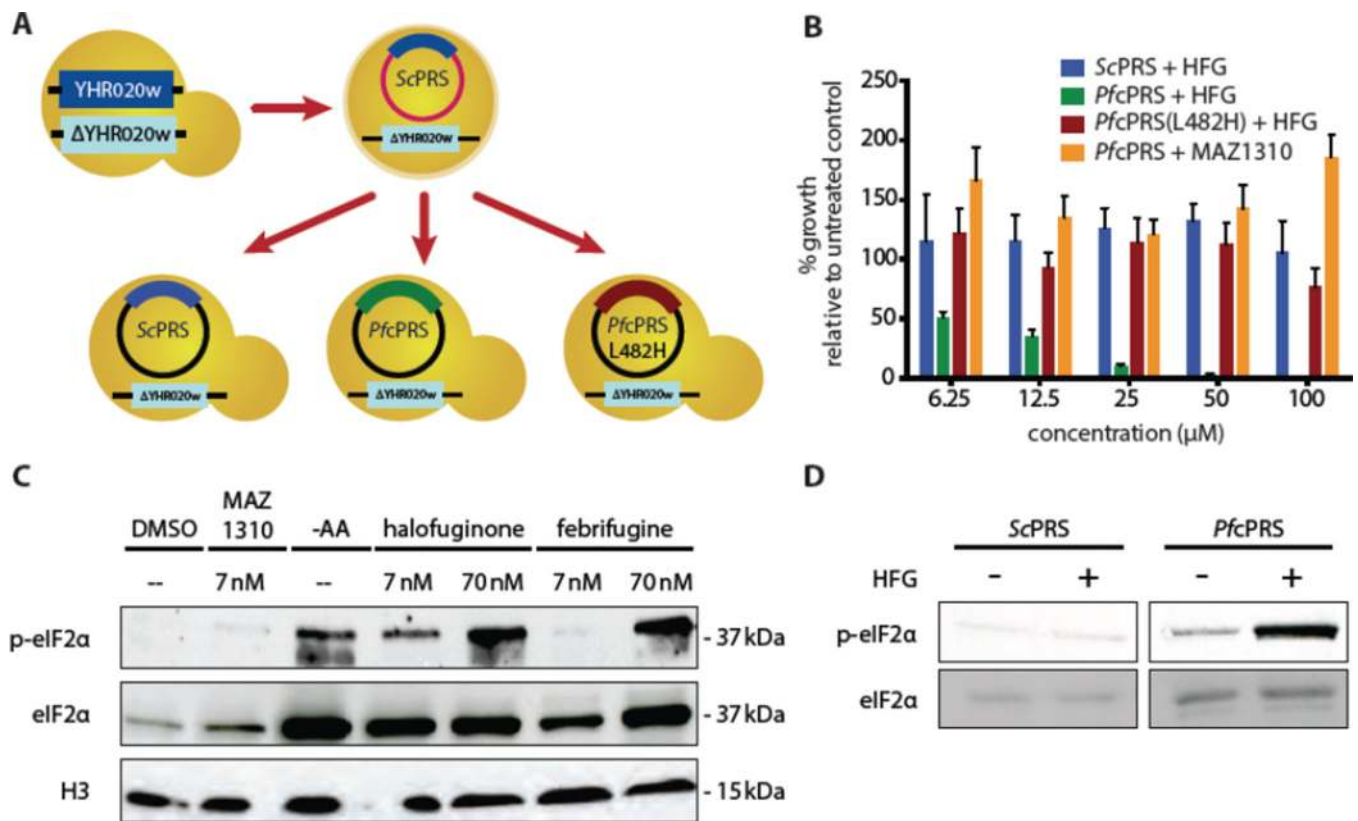


Figure 2. Confirmation of *Pf* cPRS as the functional target of halofuginone using a heterologous yeast model

(A) $+/-$ -YHR020w (*ScPRS*) heterozygous *S. cerevisiae* was transformed with a YHR020w-containing plasmid, and haploid spores were selected for genomic deletion of YHR020w. The intermediate strain was transformed with a second plasmid with an orthogonal selection marker and YHR020w, wildtype *PfcPRS* (codon optimized) or mutant *PfcPRS* (codon optimized), and subsequently selected for loss of the first plasmid. (B) Only transgenic *S. cerevisiae* expressing wildtype *PfcPRS* (green) displayed dose-dependent sensitivity to halofuginone, whereas strains expressing *ScPRS* (blue) or the L482H *PfcPRS* mutant (red) were insensitive to halofuginone treatment up to 100 μ M (all strains were *pdr1,3* deleted). The control compound MAZ1310 did not affect growth of *PfcPRS* expressing yeast (orange). (C) Halofuginone and febrifugine treatment or amino acid starvation (-AA) induce phosphorylation of eIF2 α (p-eIF2 α) after 90 minutes. Western blot analysis of phosphorylated eIF2 α and total eIF2 α protein in drug-treated asynchronous Dd2 *P. falciparum* cultures is shown. Histone H3 is the loading control and the blot is representative of two independent replicates. (D) Halofuginone (HGF) treatment induced pronounced eIF2 α phosphorylation in *PfcPRS* but not in *ScPRS*-expressing *S. cerevisiae*.

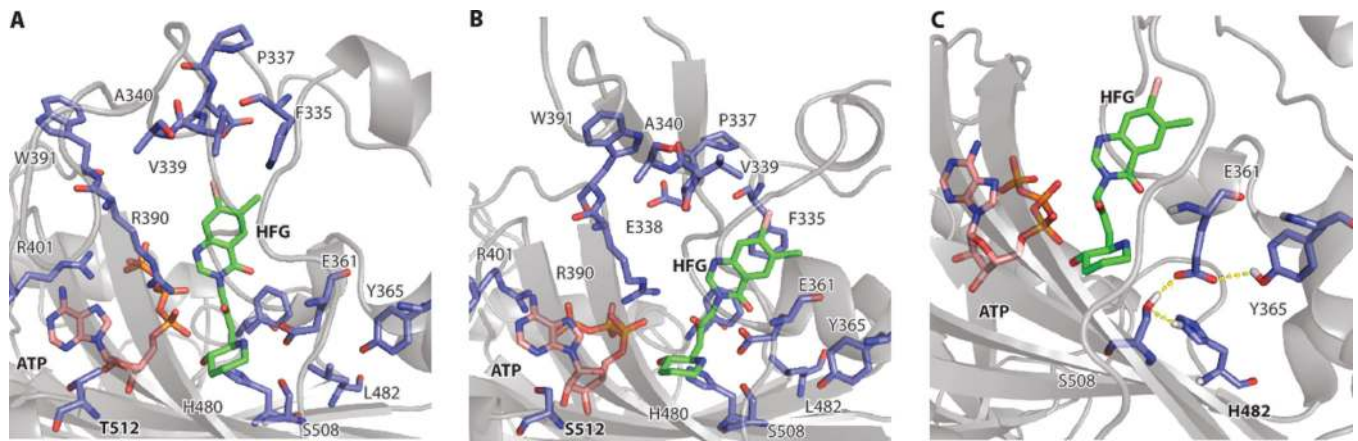


Figure 3. Models of the ternary complex of PRS with ATP and halofuginone

Shown are molecular dynamic simulations of the ternary complex of PRS with ATP and halofuginone (HFG) for: (A) the *Pfc*PRS of *P. falciparum*, (B) the *Sc*PRS of *S. cerevisiae* and (C) the *Pfc*PRS L482H mutant of *P. falciparum*. The differential binding affinity of halofuginone to *Pfc*PRS and *Sc*PRS can be traced to a T512S mutation in *Sc*PRS that results in a differential ATP binding geometry. This modification in turn changes the interaction of ATP with halofuginone and results in a reorientation of the loop consisting of residues 318–337. Specifically, F335, which stacks against the aromatic ring of halofuginone, is in a different position in the two structures. Additionally, the position of the triphosphate is different, which in turn changes the orientation of Arg401. (C) Effect of the L482H resistance mutation on the interactions of halofuginone in the active site of *Pfc*PRS. Leu482 is adjacent to the proline binding pocket, and although it does not directly participate in the hydrogen bond network formed between halofuginone and *Pfc*PRS, it does support the binding geometry of the amino acid residues that directly interact with halofuginone. The histidine in the L482H mutant provides an alternative hydrogen bond acceptor, thus destabilizing the network. All residues are numbered based on *Pfc*PRS.

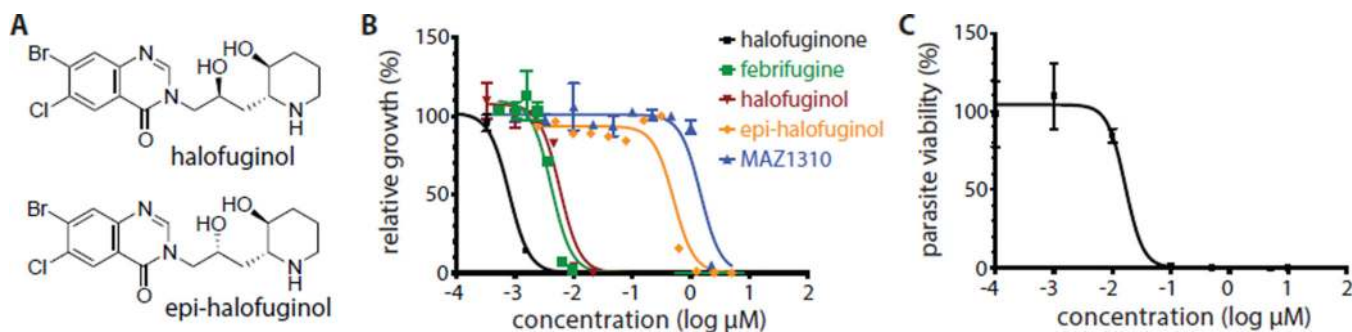


Figure 4. Halofuginol is active against the asexual erythrocytic and liver stages of the malaria parasite *in vitro*

(A) Chemical structures of halofuginol (relative stereochemistry), and epi-halofuginol (relative stereochemistry). (B) *In vitro* activity of halofuginone, febrifugine, MAZ1310, halofuginol, and epi-halofuginol against *P. falciparum* strain 3D7 erythrocytic stage parasites. Growth inhibition was quantified after 72 hours by SYBR® green staining. (C) *In vitro* dose-response for halofuginol after treatment of luciferase-expressing *P. berghei* ANKA liver stage parasites that have infected HepG2 cells.

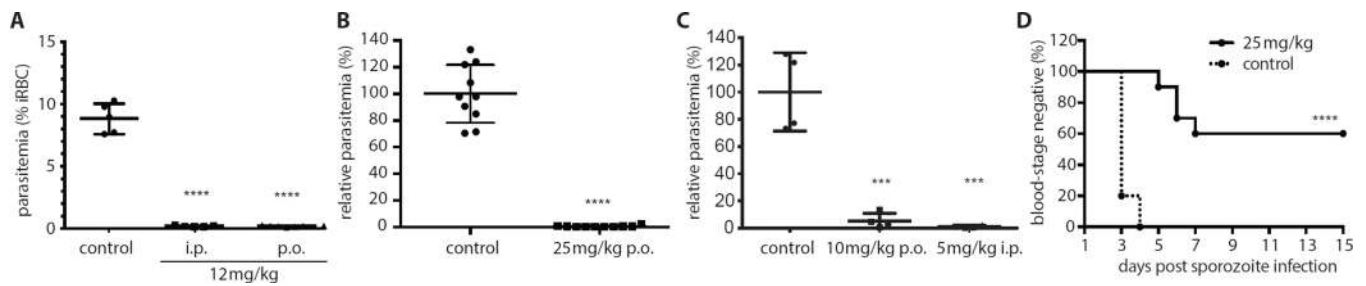


Figure 5. Halofuginol is active against the asexual erythrocytic and liver stages of the malaria parasite *in vivo*

(A) Blood parasitemia at day 5 post-infection in mice treated with halofuginol (i.p. in saline, $n = 5$; p.o. in water, $n = 7$; or vehicle, $n = 5$) q.d. for 4 days and 10 days, respectively. Treatment with halofuginol began 24 h after inoculation with 10^6 red blood cells infected with GFP-expressing *P. berghei* ANKA parasites. Blood parasite numbers were analyzed by FACS. (B) *In vivo* potency of halofuginol in the *P. berghei* mouse model of malaria. Shown is the relative parasitemia in mouse liver 44 h after infection with luciferase-expressing *P. berghei* sporozoites. Mice were treated 1 h post infection with halofuginol (25 mg/kg p.o.) or vehicle (10% hydroxypropyl-beta-cyclodextrin in 100 mM pH 5.0 citrate buffer). Parasite load was quantified relative to vehicle control by luminescence measurements. Data are displayed as mean relative to vehicle treated control, with the mean of the control group set to 100% ($n = 10$). (C) Relative parasitemia in mouse livers 44 h after infection with *P. berghei* sporozoites. Mice were treated 1hr post infection with halofuginol (i.p. in saline, p.o. in water, $n = 4$) Parasite load was quantified relative to vehicle control by qRT-PCR of *P. berghei* 18S rRNA. Data are displayed as mean relative to vehicle treated control, with the mean of the control group set to 100%. (D) Mice were maintained for 14 days post infection or until they developed blood stage malaria. Significance values (***) $p < 0.001$, **** $p < 0.0001$) were calculated (Graphpad PRISM) by ordinary one-way ANOVA (A-C) and Log-rank (Mantel-Cox) test (D).